Tetrahedron-model analysis of silicon nitride thin films and the effect of hydrogen and temperature on their optical properties

J. Petalas and S. Logothetidis
Department of Physics, Aristotle University of Thessaloniki, GR 54 006 Thessaloniki, Greece
(Received 22 November 1993; revised manuscript received 23 March 1994)

A series of silicon nitride thin films prepared by different techniques are investigated with respect to their optical properties with spectroscopic ellipsometry in the energy region 1.5–9.5 eV, using conventional and synchrotron-radiation light sources. The dielectric-function spectra of the films are analyzed with the microscopic Si-centered tetrahedron model and thus the applied growth techniques are compared, with respect to the resulting tetrahedron types and volume fractions, and the superiority of the chemical-vapor deposition techique is distinctly denoted. Moreover, a model is developed for the deduction of the films' stoichiometry from the above analysis and the results are compared with corresponding ones from Rutherford backscattering spectroscopy and elastic recoil detection. The effect of stoichiometry on the film quality and optical parameters is discussed. In addition, the effect of hydrogen on the fundamental and mean optical gaps of silicon nitride is investigated and it is concluded that in both cases hydrogen causes a shift to the red, which is interpreted as due to the existence of a significant number of Si-H bonds. Temperature-dependent optical studies on SiN bulk materials and thin films are performed in order to examine the temperature shifts of the fundamental and mean optical gaps, which are found to be redshifted and blueshifted, respectively. The effect of stoichiometry on the observed temperature coefficients is discussed.

I. INTRODUCTION

The use of amorphous wide band-gap semiconductors and insulators in miscellaneous electronic devices is nowadays extensively favored, since their electronic, optical, and mechanical properties enable operation in transistor structures[1–3] as passivating layers,[4] as well as in semiconductor multilayer structures.[5,6] Silicon nitride is the mainly studied material of this category, since its deposition on various substrates (mostly Si) can be accomplished with a variety of physical and chemical deposition methods. Moreover, the possibility of tailoring the electrical properties[7] of these films by controlling their nitrogen content and film thickness has reinforced interest in the potential technological applications of the material.

After the successful development of low-cost deposition techniques for the growth of silicon nitride films, the major task in the fabrication technology became the determination of the microstructural characteristics of the produced films and the evaluation of the quality of the product material in relation to the deposition technique and the growth conditions. In order to estimate the "perfectness" of the deposited film and its subsequent deviation from stoichiometric a-Si_3N_4, it is essential to know how the Si and N atoms are bonded. In view of the fact that the Si-centered tetrahedron model can yield a microscopic picture of the material, and in an aim to fulfill the above goal, we apply this model to our experimental data. The analysis yields information concerning the type and volume fractions of the existing Si-centered tetrahedra, and is directly related to the film homogeneity and nitrogen content. Thus the applied preparation techniques can be compared with respect to the film quality and stoichiometry produced.

The influence of hydrogen on the performance of silicon nitride electronic devices (i.e., a-Si:H/a-SiN_x:H thin-film transistors) has up to now been scarcely studied. Its effect on the dielectric and electrical properties of silicon nitride is more complicated in comparison to a-Si:H, since hydrogen can be bonded directly to either Si or N atoms and thus affects the valence-band density of states in a complex manner. For materials close to stoichiometric Si_3N_4, hydrogen is suggested to form primarily N-H bonds[8,9] and thus have a negligible influence on the location of the valence-band maximum.[10] In this work we present experimental evidence of the dependence of the fundamental and mean optical gaps of SiN_x:H on the hydrogen concentration in the material, and comment on the results.

The modification of the optical properties of crystalline materials with temperature enables an investigation of their electronic band shifts with temperature, and a subsequent check of band-structure calculations, as well as an understanding of the materials' performance in possible optoelectronic and solar device applications. In the case of amorphous materials such as silicon nitride, there exist no data in the literature on the variation over temperature of their optical properties. The temperature dependence of the fundamental gap of insulating amorphous thin films is difficult to estimate by other optical techniques, not only because the rise of the absorption is less steep than in crystalline materials and thus the optical spectra are modified by interference fringes at the region of the gap, but also because the fundamental gap location (i.e., above 4.5 eV) requires powerful vacuum ul-

traviolet (VUV) light sources, such as synchrotron radiation (SR). Therefore in the present work we report about the temperature dependence of the fundamental and mean optical gaps of silicon nitride thin films.

In Sec. II, details concerning the sample preparation and characterization and the experimental procedure will be presented. In Sec. III we shall describe the dependence of the dielectric function line shape on the silicon nitride stoichiometry (Sec. III A), refer to the tetrahedron model theory (Sec. III B) and propose a microscopic model for the estimation of stoichiometry of silicon nitride (Sec. III C). An analysis of ellipsometric data with the tetrahedron model will appear in Secs. IV A and IV B, with a discussion following in Sec. IV C. Finally, our evidence of the effect of hydrogen and temperature on the optical gaps of silicon nitride is included in Secs. V and VI, respectively, with conclusions presented in Sec. VII.

II. EXPERIMENTAL DETAILS

In this work we investigate the optical properties of a variety of silicon nitride thin films prepared by various deposition techniques, namely chemical-vapor deposition (CVD),[11] physical vapor deposition (PVD),[12,13] direct nitridation (DN),[14] plasma-enhanced CVD (PECVD), sputtering (SP),[15] and photo-CVD (Ph-CVD). The samples studied had different nitrogen concentrations, and several of them contained a significant amount of hydrogen, as will be discussed in the following sections. They were deposited on crystalline silicon substrates and their thicknesses ranged between 500 and 6000 Å. These amorphous films were characterized by the combined methods of Rutherford backscattering spectroscopy (RBS) and nuclear reaction analysis (NRA) for the determination of the individual Si, N, and O concentrations, and elastic recoil detection analysis (ERDA) for the estimation of the hydrogen content, as well as with other techniques, such as Auger sputter profiling (ASP),[14] electron microscopy, and extended x-ray-absorption fine structure (EXAFS).[15] The samples analyzed in the present work were selected among others to have low oxygen content (less than 5%). Moreover, we study some bulk, hot-pressed silicon nitride samples, prepared by sintering, which are otherwise used as targets in the PVD sputtering setup.[12,13]

In the present work the term "SiN" will be thereafter used to designate all the above-mentioned amorphous silicon-nitrogen alloys that have stoichiometries ranging between [N]/[Si]=0 (i.e., a-Si) and 1.33 (i.e., a-Si_3N_4). Therefore the term "SiN" will not indicate Si_1N_1, but will refer generally to silicon nitride materials.

The CVD films were grown by reaction of dichlorosilane and ammonia at low pressures and temperatures between 700 and 900 °C.[11] The PVD samples were deposited by sputtering of a hot-pressed SiN target with an Ar^+-ion beam at low temperatures ($\approx$30 °C).[12,13] The DN films were grown by direct exposure of (100) Si wafers to a nitrogen glow discharge at 13.56 MHz and over the temperature range 250–650 °C,[14] and are estimated by ASP to have a somewhat higher oxygen concentration, around 8%. The sputtered films were prepared by reactive sputtering in a nitrogen atmosphere, and are virtually hydrogen-free. EXAFS estimates their oxygen content to be under the detection limit of the technique[15] (i.e., less than 1%). The PECVD and Ph-CVD samples were grown by chemical reaction (f=13.56 MHz and λ=246 nm, respectively) of silane, nitrogen, and ammonia at temperatures between 150 and 390 °C, and have an oxygen content below 1.3%.

The experimental probe we applied in order to study the optical properties of the above SiN films was spectroscopic ellipsometry (SE), a nondestructive optical technique which measures directly the real and imaginary parts of the complex dielectric function $\tilde{\varepsilon}(\omega)$ $[=\varepsilon_1(\omega)+i\varepsilon_2(\omega)]$. The knowledge of the wavelength dispersion of $\varepsilon(\omega)$ provides valuable information about the materials quality and structural characteristics,[16,17] and in the case of crystalline materials about their electronic structure and density of states.[18] Analysis of the SE spectra of amorphous materials can yield the film thickness, the composition, and the location of the major optical gaps, as will be discussed in detail in the following sections.

Our SE measurements were performed in the energy region 1.5–6.3 eV using a conventional Xe lamp as a light source, and in the energy region 4.5–9.5 eV using synchrotron radiation (SR) as a light source. The respective measurements were taken at the Department of Physics of the University of Thessaloniki and at the Synchrotron Radiation Laboratory BESSY in Berlin,[19] Germany. The need for reliable light sources in the vuv region is essential in order to study the optical response of wide-band-gap materials,[20] such as SiN. Conventional visible-UV lamps present problems and have a low output power at high energies, whereas SR is an extremely powerful light source with an enormous spectral range (i.e., 3 eV–150 keV). Our SR measurements utilized the lower part of the above spectrum with the help of a 2m-Seya Namioka monochromator. In both experimental setups the angle of incidence on the samples surface was 67.5°, and the SR ellipsometric measurements were taken under high-vacuum conditions ($P<10^{-8}$ Torr). Temperature-dependent measurements were taken in the temperature range 80–700 K.

SE is a surface-sensitive experimental technique and therefore we had to take certain precautions before placing the samples in the UHV chambers. In detail, we followed a four-stage surface cleaning procedure in order to remove organic contaminants from the outer surfaces, namely heating at about 50 °C for 5 min in trichloroethylene, acetone, and methanol, and finally rinsing with deionized water. This technique is reported to be appropriate in the case of III-V and group-IV semiconductors and insulators.

III. TETRAHEDRON MODEL DEVELOPMENT

A. Relation between the nitrogen content and the dielectric function $\varepsilon(\omega)$

Amorphous silicon (a-Si) is formed by the interaction of the tetrahedrally coordinated sp^3 hybrid orbitals of Si.

The electronic transitions to antibonding, conduction-band states in the material originate from the Si $3p$ levels. The mean separation between the valence and conduction bands, known as the mean optical gap E_0, represents the average distance between the center of gravity of the density of states (DOS) of the valence and conduction bands.[10,21] This magnitude is directly observable in the ellipsometric data, since the imaginary part $\varepsilon_2(\omega)$ of the dielectric function presents (3.8 eV) a maximum at this energy, hereafter denoted as ε_{2max}.

The incorporation of N atoms in a-Si causes the interaction of the Si sp^3 hybrids with N sp^2 ones, and alters the shape of the valence-band (VB) DOS (Fig. 1, after Ref. 21). Transitions from the nitrogen $2p_z$ levels start to contribute to the mean optical gap and therefore the center of gravity of the VB DOS is lowered, since the N $2p_z$ states lie lower than the Si $3p$ ones. Hence E_0, and consequently ε_{2max}, are shifted to higher energies. The more the percentage of Si-N bonds in the material, the greater the shift. For [N]/[Si] greater than unity, the N $2p_{xy}$ states, lying below the N $2p_z$ ones, are also thought to contribute to the shift of E_0 and ε_{2max} to even higher energies.[21] For the extreme case where all Si-Si bonds are replaced by Si-N ones, and Si_3N_4 material is formed, ε_{2max} is located at around 9.6 eV. Therefore, the energy position of ε_{2max} is directly associated with the nitrogen content in SiN material.

Similar observations can be made about the real part $\varepsilon_1(\omega)$ of the dielectric function, whose major peak, ε_{1max} occurs at 2.8 and 7.0 eV for the cases of a-Si and a-Si_3N_4, and is also indicative of the material stoichiometry. For instance, in Figs. 2(a) and 2(b) we present the real and imaginary parts of the dielectric function of several SiN thin films deposited by different techniques, as well as the $\tilde{\varepsilon}(\omega)$ data of a-Si and a-Si_3Ni_4 found in the literature.[22,23] One should not be misled by the interference fringes which are present in the lower-energy part of certain ε_1 and ε_2 spectra, and which somewhat distort the overall line shape. These fringes are due to the multiple reflection of light between the film surface and the film-substrate interface, and convey information about both the film and the substrate. A methodology that can extract the above fringes from the measured spectra and thus reveal the optical response of the SiN film solely is described in the Appendix.

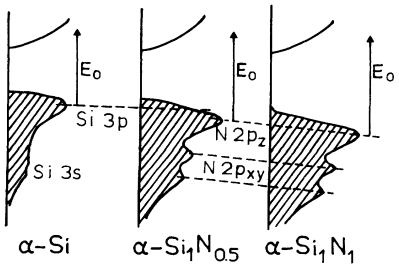

FIG. 1. The modification of the valence-band DOS of a-Si due to the incorporation of nitrogen atoms and the formation of SiN_x (after Ref. 21).

From Figs. 2(a) and 2(b) and in conjunction with the preceding paragraphs, it is clearly seen that the SiN films under consideration contain different amounts of nitrogen, with the closest to stoichiometric being the sputtered (SP) film. The differences between the absolute values of the ε_{1max} and ε_{2max} of the films presented in Figs. 2(a) and 2(b) are easily explainable, since it is well known that apart from the stoichiometry the presence of voids (i.e., density deficit), surface roughness, and structural imperfections (dislocations, twins, etc.) are all causes for the degradation of the absolute values of $\varepsilon_1(\omega)$ and $\varepsilon_2(\omega)$.[24]

B. The tetrahedron model for SiN and SiN:H

Amorphous Si is bonded tetrahedrally, and is thought to be comprised entirely of tetrahedra of the type $Si\text{-}Si_4$.[25]

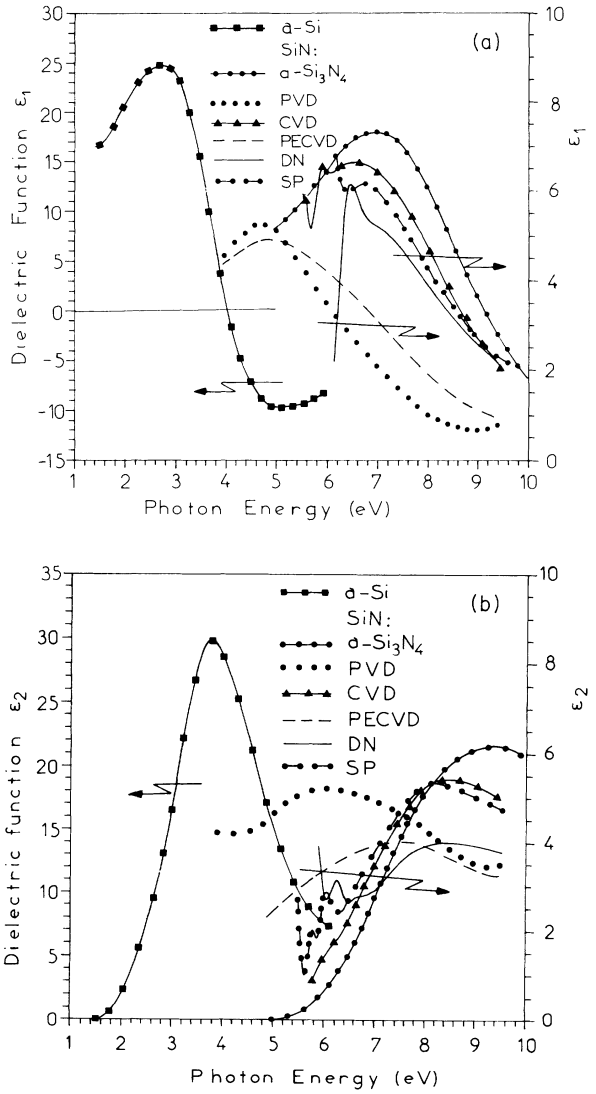

FIG. 2. (a) The real (ε_1) part of the dielectric function of a-Si, a-Si_3N_4 and various SiN samples. Note that the left-hand scale corresponds to a-Si, and that the right-hand scale to a-Si_3N_4 and all SiN films. (b) As in (a), the imaginary (ε_2) part of the dielectric function.

The deposition of nitrogen atoms on an a-Si surface causes the incorporation of N into these tetrahedra. In order to describe the structural changes in such a system we employ the microscopic Si-centered tetrahedron model, which supposes the formation of tetrahedra of the type $Si\text{-}Si_{4-v}N_v$, where $v=0$, 1, 2, 3, and 4.[26] These five units, comprised of all the various combinations of Si-Si and Si-N bonds, are thought to constitute the material, and therefore the model can be applied correctly only to Si-rich SiN. When all Si-Si bonds are replaced by Si-N ones, the material is thought to consist of $Si\text{-}N_4$ tetrahedra entirely and its synthesis becomes Si_3N_4; that is, stoichiometric a-Si_3N_4.

The dielectric response of a-Si (i.e., $Si\text{-}Si_4$ tetrahedron) is well known in the visible and near-UV regions.[22] Aspnes and Theeten[26] proposed a method ("scaling approach") with which the individual dielectric responses of the rest $Si\text{-}Si_{4-v}N_v$ tetrahedra can be calculated ($v=1,\ldots,4$) from the dielectric function of a-Si. In addition, theory predicts that for a given stoichiometry x the tetrahedron probabilities P_v in a Si_xN_{1-x} material ($0.43<x<1$) can be precisely estimated and therefore the dielectric function of the material can be theoretically calculated. Following the formalism explicitly described in Ref. 27, the existence probabilities f_1 and f_2 of the Si-Si and Si-N bonds are

$$f_1=\frac{7x-3}{4x} \quad \text{and} \quad f_2=\frac{3(1-x)}{4x} \ . \tag{1}$$

Note that for $x=1$ (a-Si) we obtain $f_1=1$ and $f_2=0$, whereas for $x=\frac{3}{7}$ (a-Si_3N_4) we obtain $f_1=0$ and $f_2=1$, as expected.

If homogeneous dispersion of the bonds in the material [random-bonding (RB) model] is considered, the tetrahedron probabilities P_v are given by the formula

$$P_v=\frac{4!f_1^{4-v}f_2^{v}}{(4-v)!v!} \ . \tag{2}$$

Since the Si-Si and Si-N bond lengths are different (1.176 and 0.867 A,[26] respectively), in order to calculate the volume fraction u_v of each tetrahedron in the material one should also consider the individual volumes V_v of the tetrahedra, in the manner described extensively in Ref. 27. On the other hand, if the material is assumed to consist of separate a-Si and a-Si_3N_4 regions, i.e., solely from $Si\text{-}Si_4$ and $Si\text{-}N_4$ tetrahedra [phase separation (PS) model], the tetrahedron probabilities are simplified as follows: $P_0=f_1$, $P_1=P_2=P_3=0$, and $P_4=f_2$.

With the above analysis the volume fractions u_v of the five $Si\text{-}Si_{4-v}N_v$ tetrahedra can be obtained for given stoichiometry x and therefore the dielectric functions $\varepsilon_v(\omega)$ calculated with the scaling approach can be combined accordingly, with the help of the Bruggeman effective-medium theory (EMT):[28]

$$\sum_{v=0}^{4}\frac{\varepsilon_v(\omega)-\langle\varepsilon(\omega)\rangle}{\varepsilon_v(\omega)+2\langle\varepsilon(\omega)\rangle}u_v=1 \quad \text{where} \quad \sum_{v=0}^{4}u_v=1 \ . \tag{3}$$

In the above equation $\langle\varepsilon(\omega)\rangle$ is the resulting dielectric function of the Si_xN_{1-x} material. For instance, in Figs. 3 and 4 we present the calculated imaginary part $\varepsilon_2(\omega)$ of the dielectric function of Si_xN_{1-x} materials with varying N content for the case of the RB and PS models, respectively. As seen in Figs. 3 and 4, in the RB approach $\varepsilon_2(\omega)$ presents a single peak, but in the PS approach the structure is more complicated. For low and high nitrogen contents one peak is evident (that of the respective dominant phase), but for intermediate N concentrations two peaks can be detected.

The incorporation of hydrogen atoms in a-Si can be studied with the tetrahedron model by considering the substitution of Si-Si bonds with Si-H ones, and developing an appropriate formalism.[29] A tetrahedron-model analysis of the dielectric function involves four $Si\text{-}Si_{4-v}H_v$ tetrahedra.[30] However, for the case of amorphous hydrogenated silicon nitride the tetrahedron consideration becomes more complex, since three elements should be involved in the Si-centered tetrahedra and a variety of bonds can be formed. Hence one can consider that hydrogen atoms can be bonded only to nitrogen atoms, which forbids the existence of Si-H bonds. Since it is still difficult to deal with three types of bonds (Si-Si, Si-N and N-H), one can further consider N-rich material, where the existence probability of the Si-Si bond is scarce, and therefore involve only Si-N and N-H bonds in the model. This model can be applied only in the case of stoichiometric SiN films ($[N]/[Si]\approx 1.30$), so that on the one hand no Si atoms are present at the tetrahedron corners, which are entirely occupied by N atoms, and on the other hand no N-N bonds are formed, due to excess N. The preferential formation of heteronuclear bonds is also known as chemical ordering.[31]

The material can be designated as $Si_xN_yH_z$ or $Si_xN_{y-z}(NH)_z$, since hydrogen is bonded to nitrogen only and thus forms (NH) units. Five bonding units constitute such a material, namely the $Si\text{-}N_{4-v}(NH)_v$ tetrahedra ($v=0,1,\ldots,4$) of probabilities P_v. Following the formalism presented in Ref. 27, the existence proba-

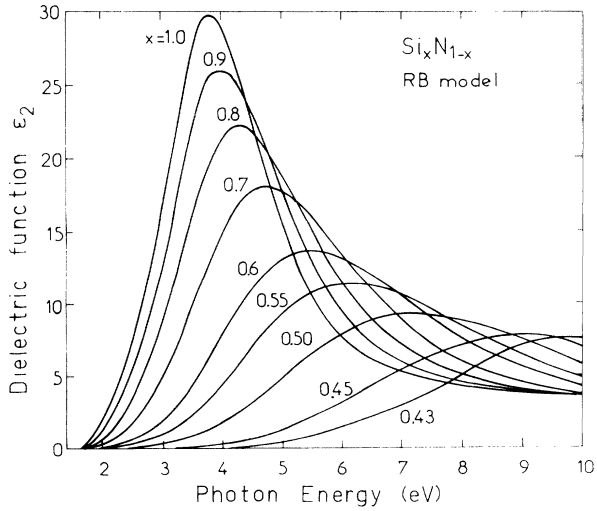

FIG. 3. The imaginary part of the dielectric function of Si_xN_{1-x} materials, as calculated from the EMT combination of $Si\text{-}Si_{4-v}N_v$ tetrahedra considering the random bonding model.

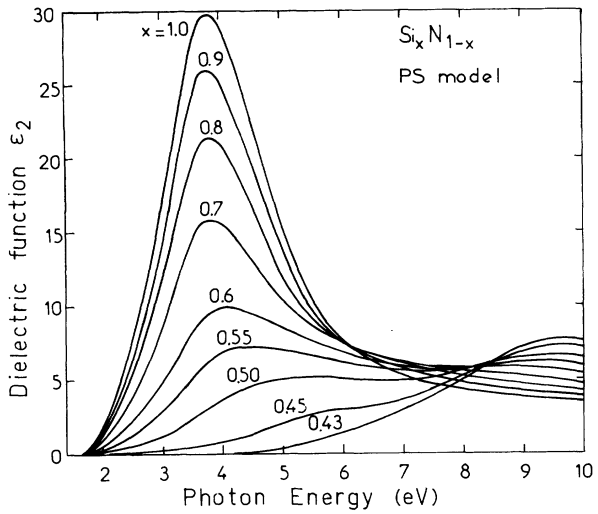

FIG. 4. The imaginary part of the dielectric function of Si_xN_{1-x} materials, as calculated from the EMT combination of $Si\text{-}Si_{4-v}N_v$ tetrahedra considering the phase-separation model.

bilities f_1 and f_2 of the Si-N and N-H bonds are

$$f_1=\frac{3(y-z)}{4x} \quad \text{and} \quad f_2=\frac{z}{2x} \ . \tag{4}$$

The tetrahedron probabilities P_v of the five tetrahedra are given by Eq. (2) for the case of the RB model.

C. Stoichiometry estimation from given volume fractions

In an effort to relate the tetrahedron-model predictions for the dielectric function of SiN with the ellipsometric data on SiN films, we aim to fit experimental dielectric-function spectra, considering various combinations of $Si\text{-}Si_{4-v}N_v$ [and $Si\text{-}N_{4-v}(NH)_v$, where appropriate] tetrahedra using Eq. (3). Such a fitting procedure can determine the volume fractions of the existing tetrahedra plus a volume fraction for the voids present in the material. In the term "void fraction" are accumulated all density deficits that are due to imperfections, like defects, small surface roughness, or hydrogen bonds with small polarizability, which are not taken into account in this model. Hence a formalism has to be developed, in order to calculate the [N]/[Si] ratio and the hydrogen content H% for given tetrahedron volume fractions.

The model proposed in this paragraph requires one basic assumption, namely that all electrons of the Si, N, and H atoms participate in chemical bonds. By definition, in the following analysis the five tetrahedra of the type $Si\text{-}Si_{4-v}N_v$ ($v=0$, 1, 2, 3, and 4) will be called $T0$, $T1$, $T2$, $T3$, and $T4$, according to their content in nitrogen atoms, whereas the $Si\text{-}N_{4-v}(NH)_v$ tetrahedra will be denoted as $T0H$, $T1H$, $T2H$, $T3H$, and $T4H$, depending on their content in hydrogen atoms. Note that the tetrahedra $T4$ and $T0H$ are identical. The model counts the number of Si, N, and H atoms that belong to a certain tetrahedron, and thus counts the total fractions of Si, N, and H atoms in the material.

Every Si atom in a silicon nitride material forms tetrahedral bonds and is located in the center of a tetrahedron, at the corners of which other Si or N atoms are situated. The former are at the center of their own tetrahedra. For a proper representation consistent with EMT, a SiN_x material has to be considered as a number of tetrahedra that are bonded together by having corner atoms in common. In this way the tetrahedra do not intersect and overlap each other and hence an EMT analysis can be applied to them, since EMT regards the material as consisting of a number of phases (in our case the Si-centered tetrahedra) that have their own dielectric identity, i.e., they exhibit a specific dielectric response. Therefore the total dielectric response of the system is obtained by EMT from the individual responses of these tetrahedra, and some Si atom is either at the center or corner of one of these. It follows that the total number of tetrahedra considered in the EMT calculation is equal to the number of Si atoms situated at tetrahedron centers. For example, it can be shown that every $Si\text{-}Si_4$ tetrahedron is bonded to other 12 tetrahedra, whereas every $Si\text{-}N_4$ tetrahedron is bonded to other eight tetrahedra.

At the four corners of each tetrahedron there exist Si, N, or H atoms, depending on the specific tetrahedron. One Si atom located at a corner of a certain $Si\text{-}Si_{4-v}N_v$ tetrahedron is expected to participate to other three tetrahedra as corner atom, since Si has four valence electrons, and therefore its contribution to the tetrahedron under consideration is $\frac{1}{4}$ atoms. In the same manner, one nitrogen atom located at a corner of a certain tetrahedron and not being bonded to a hydrogen atom forms three Si-N bonds, and hence participates in other two tetrahedra; its contribution to each of the three tetrahedra is therefore $\frac{1}{3}$ atoms. Nitrogen atoms bonded to hydrogen have two electrons available to bond to Si, and therefore such an atom contributes to a certain tetrahedron by the factor $\frac{1}{2}$. Finally, one hydrogen atom participates in a certain tetrahedron by the factor $\frac{1}{2}$, since the (NH) unit is bonded to two tetrahedra.

Therefore, in order to determine the Si, N, and H atom fractions x, y, and z, respectively, from the tetrahedron volume fractions u_i, the tetrahedron fractions P_i have to be determined first. The magnitudes u_k for s tetrahedra are defined as[27]

$$u_k=\frac{P_kV_k}{\sum_i P_iV_i}, \quad i=1,\ldots,s$$

$$\text{where } \sum_i u_i=1 \text{ and } \sum_i P_i=1 \ , \tag{5}$$

where V_i represents the tetrahedron volumes. If u_k represents the experimentally estimated tetrahedron volume fractions, the above homogeneous system of equations must be solved with respect to tetrahedron fractions P_k. Therefore we obtain

$$P_k=\frac{u_k}{V_k}\Big/\sum_{i=1}^{s}\frac{u_i}{V_i}, \quad k=1,2,\ldots,s \ . \tag{6}$$

The atom fractions x, y, and z can be defined from the total numbers of Si, N, and H atoms as follows:

$$x = \mathrm{N(Si)/N(total)} = \mathrm{N(Si)/[N(Si)+N(N)+N(H)]} , \tag{7a}$$

$$y = \mathrm{N(N)/N(total)} , \tag{7b}$$

$$z = \mathrm{N(H)/N(total)} . \tag{7c}$$

Hence, in the general case where all nine tetrahedra ($T0$, $T1$, $T2$, $T3$, $T4$, $T1H$, $T2H$, $T3H$, and $T4H$) are considered to have fractions P_{T0}, P_{T1}, P_{T2}, P_{T3}, P_{T4}, P_{T1H} P_{T2H}, P_{T3H}, and P_{T4H}, respectively, the number of Si, N, and H atoms at specific tetrahedron sites is as follows.

Si atoms at tetrahedron centers:

$$K = P_{T0}+P_{T1}+P_{T2}+P_{T3}+P_{T4} + P_{T1H}+P_{T2H}+P_{T3H}+P_{T4H} .$$

Si atoms at tetrahedron corners:

$$(4P_{T0}+3P_{T1}+2P_{T2}+P_{T3})/4 .$$

N atoms at tetrahedron corners (not bonded to hydrogen):

$$(P_{T1}+2P_{T2}+3P_{T3}+4P_{T4})/3+(3P_{T1H}+2P_{T2H}+P_{T3H})/3.$$

N atoms at tetrahedron corners (bonded to hydrogen):

$$(P_{T1H}+2P_{T2H}+3P_{T3H}+4P_{T4H})/2 .$$

H atoms in (NH) units:

$$(P_{T1H}+2P_{T2H}+3P_{T3H}+4P_{T4H})/2 .$$

Therefore, the total number of Si, N, and H atoms in the $\mathrm{Si}_x\mathrm{N}_y\mathrm{H}_z$ material are proportional to the quantities

$$x' = K + \frac{4P_{T0}+3P_{T1}+2P_{T2}+P_{T3}}{4} , \tag{8a}$$

$$y' = \frac{P_{T1}+2P_{T2}+3P_{T3}+4P_{T4}}{3} + \frac{9P_{T1H}+10P_{T2H}+11P_{T3H}+12P_{T4H}}{6} , \tag{8b}$$

$$z' = \frac{P_{T1H}+2P_{T2H}+3P_{T3H}+4P_{T4H}}{2} , \tag{8c}$$

and thus the atom fractions are

$$x = x'/(x'+y'+z') , \tag{9a}$$

$$y = y'/(x'+y'+z') , \tag{9b}$$

$$z = z'/(x'+y'+z') . \tag{9c}$$

The formalism of the above model is summarized in Table I.

IV. TETRAHEDRON-MODEL ANALYSIS OF ELLIPSOMETRIC DATA

A. Analysis method

As already discussed, the tetrahedron model associates the optical response of materials (i.e., the dielectric function) with their microscopic structure and especially with the type and nature of the existing bonds. In order to investigate the above for the case of SiN thin films, the complex dielectric functions of the individual $\mathrm{Si\text{-}Si}_{4-v}\mathrm{N}_v$ [and $\mathrm{Si\text{-}N}_{4-v}(\mathrm{NH})_v$, where appropriate] tetrahedra, determined from the formalism described in Sec. III B, are combined with the use of EMT [Eq. (3)]. Our objective is to determine the volume fractions u_v of the existing tetrahedra and thus fit the $\tilde{\varepsilon}(\omega)$ experimental spectra considering all possible combinations of the above-mentioned tetrahedra. As noted in Sec. III A, a significant factor that tunes the $\tilde{\varepsilon}(\omega)$ line shape is the number of voids in the film. Since the dielectric response of voids at energies up to at least 6 eV is well known ($\tilde{\varepsilon}_{\mathrm{voids}} = 1+i0$), a void term of this type is assumed for the whole measurement region (up to 9.5 eV) and is thus included in Eq. (3) for a proper representation of the material.

The energy region of the $\tilde{\varepsilon}(\omega)$ spectra which is being fitted is up to 9.5 eV, which is the energy limit of our experimental setup. As described in Sec. III A, interference fringes are superimposed on the lower-energy part of the SiN film spectra, since the materials under study are transparent in the visible and therefore the penetrating light is multiply reflected at the film/substrate interface. Nearby the fundamental gap though, the penetration depth of the light diminishes and the amplitude of these

TABLE I. The formalism developed for the estimation of the Si, N, and H content of $\mathrm{Si}_x\mathrm{N}_y\mathrm{H}_z$ films containing $\mathrm{Si\text{-}Si}_{4-v}\mathrm{N}_v$ and $\mathrm{Si\text{-}N}_{4-v}(\mathrm{NH})_v$ tetrahedra at given tetrahedron fractions.

Tetrahedron		Tetrahedron fraction	Si		N		H
			center	corner	=N—	=NH	=NH
$T0$	$\mathrm{Si\text{-}Si}_4$	P_{T0}	P_{T0}	$4P_{T0}/4$	0	0	0
$T1$	$\mathrm{Si\text{-}Si}_3\mathrm{N}$	P_{T1}	P_{T1}	$3P_{T1}/4$	$P_{T1}/3$	0	0
$T2$	$\mathrm{Si\text{-}Si}_2\mathrm{N}_2$	P_{T2}	P_{T2}	$2P_{T2}/4$	$2P_{T2}/3$	0	0
$T3$	$\mathrm{Si\text{-}SiN}_3$	P_{T3}	P_{T3}	$P_{T3}/4$	$3P_{T3}/3$	0	0
$T4$	$\mathrm{Si\text{-}N}_4$	P_{T4}	P_{T4}	0	$4P_{T4}/3$	0	0
$T1H$	$\mathrm{Si\text{-}N}_3(\mathrm{NH})$	P_{T1H}	P_{T1H}	0	$3P_{T1H}/3$	$P_{T1H}/2$	$P_{T1H}/2$
$T2H$	$\mathrm{Si\text{-}N}_2(\mathrm{NH})_2$	P_{T2H}	P_{T2H}	0	$2P_{T2H}/3$	$2P_{T2H}/2$	$2P_{T2H}/2$
$T3H$	$\mathrm{Si\text{-}N(NH)}_3$	P_{T3H}	P_{T3H}	0	$P_{T3H}/3$	$3P_{T3H}/2$	$3P_{T3H}/2$
$T4H$	$\mathrm{Si\text{-}(NH)}_4$	P_{T4H}	P_{T4H}	0	0	$4P_{T4H}/2$	$4P_{T4H}/2$
		K	x'		y'		z'

fringes decreases gradually. Therefore, the lower-energy limit of our fittings is selected to occur slightly after the disappearance of interference fringes. The mean-square deviation between experiment and fit represents the criterion for determining the best fits.

RBS/NRA and ERDA measurements on all films, listed in the first and fourth columns of Table II, estimate that the CVD, DN, and SP films under study are close to stoichiometric ([N]/[Si] ranges between 1.15 and 1.3), oxygen free, and with a very low hydrogen content (1–5 %). Such low hydrogen content is difficult to detect by the tetrahedron-model fitting of the dielectric function, and therefore fittings involving Si-$Si_{4-v}N_v$ tetrahedra are applied in these cases. In Fig. 5 we present the fit results in the case of two SiN samples, namely the low-[N]/[Si] PVD3 and hydrogen-rich Ph-CVD film. The solid lines designate the experimental dielectric-function spectra, whereas the dashed lines the corresponding best fits, whose results (volume fractions) are presented in Table III.

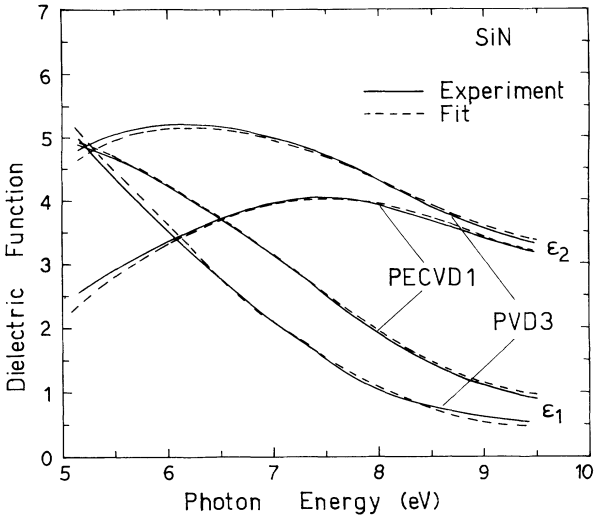

FIG. 5. Typical fittings of the experimental dielectric-function spectra of silicon nitride thin films (solid lines) with the model described in Sec. IV A and with the help of Eq. (3) (dashed lines).

TABLE II. The [N]/[Si] ratio and H concentration for all SiN films studied determined by RBS/NRA, IR, and ERDA, and compared to those found from ellipsometry (SE) and tetrahedron-model (TM) analysis.

	[N]/[Si]			H(%)		
	Experimental		Theoretical	Experimental		Theoretical
	RBS/NRA	SE	TM	IR	ERDA	TM
PVD1	1.0	1.00	0.84		17	
PVD2	1.0	1.05	0.85		17	
PVD3	1.0	0.82	0.67		8	
PVD4	1.0	0.97	0.85		8	
PVD5	1.0	0.98	0.86		5	
PVD6	1.0	0.93	0.72		7	
PVD7	1.0	0.55	0.46		7	
CVD0	1.3	1.14	1.12		2.5	
CVD1	1.3	1.17	1.21		2.0	
CVD2	1.3	1.15	1.16		6.2	
CVD3	1.3	1.16	1.16		4.7	
CVD4	1.27	1.16	1.15		5.0	
CVD5	1.17	1.12	1.02		2.5	
DN1			1.09			
DN2	1.2	1.16	1.18		1.25	
DN3	1.29	1.20	1.25		1.7	
SP1		1.13	1.10			
SP2	1.3	1.14	1.10		5.2	
SP3	1.17	1.13	1.18		5.9	
SP4	1.27	1.19	1.16		6.6	
PECVD1	0.95	1.04	0.82	10	22.6	9.3
PECVD2	1.3	1.12	1.03	8	16	12.0
Ph-CVD	1.25	1.12	1.00	10	26.6	13.1

B. Results

1. PVD SiN films

RBS/NRA studies[12] estimate the PVD SiN films to be Si-rich ([N]/[Si] =1.0), whereas ERDA (Ref. 13) measurements determine a significant hydrogen concentration of 7–15 % (see Table II). Hence the number of Si-H bonds in the material must be important, and therefore the consideration of Si-$N_{4-v}(NH)_v$ tetrahedra in the film is not appropriate. Therefore we selected to fit the PVD films accounting for only Si-$Si_{4-v}N_v$ tetrahedra, expecting that the presence of hydrogen would cause at least an overestimation of the void fraction.

The best fittings in the case of all PVD SiN/Si films are obtained for the tetrahedron combination $T1+T2+T4$ (see Table III for results). All these films were rather far from stoichiometric, so the inclusion of $T1$ in the best fit is reasonable; this tetrahedron is found to finely tune the fitting curve toward experiment. In addition, all fittings which contain $T2$ are by far better than the corresponding ones which contain $T3$; this implies that $T2$ is necessary for the description of the PVD films, and that its contribution cannot be successfully substituted with a joint contribution of $T1$ and $T3$. Typical results obtained from the best fits of PVD samples are $u_1=4\%$, $u_2=25\%$, $u_4=40\%$, and $u_{\text{voids}}=31\%$. The void fraction estimated by the best fits ranges from 28% to 37%; the latter value is rather large and the sample that yields $u_{\text{voids}}=37\%$ exhibits a very low $\varepsilon_{2\max}$ energy position (6.7 eV). The void fraction, as already discussed in Sec. III, represents a number of deficiencies in the material, cannot entirely be attributed to density deficit, and therefore is indicative in this case of inferior film quality.

We also measured PVD SiN/C (sample PVD7, Tables II and III), which should be treated as a special case not only because it presented the only successful fit consider-

TABLE III. Composition and stoichiometry of various SiN films, as determined from the tetrahedron-model analysis of the dielectric function by considering $Si\text{-}Si_{4-v}N_v$ tetrahedra.

	Tetrahedron volume fractions (%)					Void fraction	Atom fractions (%)		
	$T0$	$T1$	$T2$	$T3$	$T4$	(%)	Si	N	[N]/[Si]
PVD1		6.6	32.5		60.9	28.3	54.3	45.7	0.84
PVD2		11.6	23.6		64.8	31.0	54.0	46.0	0.85
PVD3		19.8	33.2		47.0	31.7	54.9	40.1	0.67
PVD4		4.2	35.2		60.6	29.5	54.1	45.9	0.85
PVD5		1.2	39.8		59.0	32.7	53.9	46.1	0.86
PVD6		15.3	33.7		51.0	37.1	58.2	41.8	0.72
PVD7	23.3	12.9	24.6		39.2	39.5	68.3	31.7	0.46
CVD0			2.4	29.0	68.6	29.0	47.2	52.8	1.12
CVD1				18.7	81.3	16.2	45.2	54.8	1.21
CVD2			1.4	24.2	74.4	21.1	46.3	53.7	1.16
CVD3			0.5	25.1	74.4	21.2	46.2	53.8	1.16
CVD4			4.0	19.8	76.2	19.7	46.5	53.5	1.15
CVD5			18.5	12.3	69.2	31.5	49.4	50.6	1.02
DN1			18.3		81.7	29.9	47.8	52.2	1.09
DN2			10.9		89.1	27.2	45.8	54.2	1.18
DN3			6.0		94.0	31.4	44.5	55.5	1.25
SP1		4.7	10.5		84.8	37.9	47.7	52.3	1.10
SP2		1.0	16.4		82.6	37.3	47.7	52.3	1.10
SP3			11.3		88.7	12.0	45.9	54.1	1.18
SP4			12.4		87.6	17.2	46.2	53.8	1.16

ing four tetrahedra, namely the combination $T0+T1+T2+T4$, but also because of its extremely low ε_{2max} energy position (6.0 eV), while in all PVD SiN/Si samples the location of ε_{2max} ranged between 6.5 and 7.5 eV. The latter is an indication of an unsatisfactory nitrogen deposition, and influences the corresponding best-fit results. In detail, its tetrahedron-volume fractions are $u_0=23\%$, $u_1=12.9\%$, $u_2=24.6\%$, $u_4=39.2\%$, and $u_{voids}=39.5\%$ (Table III). Although $u_1<u_2<u_4$, a result consistent with the RB model predictions, the fact that u_0 is significantly higher than u_1 and comparable to u_2 indicates that the RB model approximation cannot satisfactorily represent this sample, and that a significant PS phase must be existent. This may be due to nonhomogeneous deposition of N on the carbon surface.

2. *CVD SiN films*

The CVD SiN films CVD0-3, CVD4, and CVD5 were obtained, respectively, from three different sources, and their ε_{2max} energy position ranged between 8.1 and 8.5 eV. Best fits were obtained by the tetrahedron combination $T2+T3+T4$ or $T3+T4$, as listed in Table III. The percentage of the $T2$ tetrahedron is negligible in the cases of all but one film, and thus helps to tune the fitting. The $T4$ tetrahedron is found to be predominant in the material, and the ratio u_3/u_4 ranges between 0.23 and 0.42. A further study of possible combinations between $T2$, $T3$, and $T4$ indicates that these tetrahedra do not yield best fits accidentally. Moreover, in contrast to other types of samples, no feasible fitting involving the $T1$ tetrahedron was achieved. The ratios between the tetrahedron-volume fractions are indicative of a randomly bonded material, and the void fraction is found to be relatively low (between 16 and 29%).

In only one case (sample CVD5) does the presence of Si-rich tetrahedra become important. This is in agreement with the dielectric-function line shape, where $\varepsilon_{2max}=8.1$ eV, which indicates a relatively low nitrogen content. Moreover, the bets fit estimates that $u_2>u_3$ (Table III), a result suggesting a nonhomogeneously deposited material. The fact that this sample exhibits the highest void volume fraction (31.5%) in comparison to the other CVD films is in accordance with the above argument.

Therefore, from all the above the CVD technique seems to cause gradual nitridation of the a-Si matrix and thus produce good quality SiN material. Moreover, the network appears to be randomly bonded with homogeneously dispersed Si-Si and Si-N bonds. In view of the fact that this is the only sample category in which the tetrahedron combination $T2+T3+T4$ yields best fits, one may also suppose that this combination is characteristic of the CVD method itself.

3. *DN SiN films*

Best-fit results are obtained with the combination $T2+T4$ in the case of DN SiN films (see Table III). The material is found to consist predominantly of the $T4$

tetrahedron, since the volume fraction u_4 is estimated to range between 82 and 94%. Although all films are close to stoichiometric, with the ε_{2max} energy position located above 8.4 eV, no feasible fit could be obtained by the tetrahedron combination $T2+T3+T4$. This may indicate the absence of the $T3$ tetrahedron in the material, and could be associated with the relatively high estimated void fraction (around 30%). Fittings considering the tetrahedron combinations $T3+T4$ and $T1+T3+T4$ are also viable for all DN samples.

4. SP SiN films

The sputtered SiN films SP1-2 and SP3-4 were obtained, respectively, from two sources. Both kinds of samples were of high nitrogen content, as deduced from their ε_{2max} location (between 8.5 and 8.65 eV). The results of their tetrahedron-mode analysis are listed in Table III. In all cases the $T4$ tetrahedron is predominant (u_4 ranges between 82.6% and 88.7%). The best fit is attained by also considering a volume fraction of the $T2$ tetrahedron. In two cases a small percentage of the $T1$ tetrahedron is also necessary (4.7% and 1.0%, respectively) for a fine tuning of the fit. These samples exhibit a void fraction of around 37.6%, which is rather much for materials of high u_4 volume fraction, and suggests that the film quality is not very high. On the other hand, the other two films exhibit significantly lower void fractions (12% and 17%, respectively), which may be indicative of higher quality. Therefore, in the case of the sputtered films the tetrahedron-model analysis indicates the presence of tetrahedra $T2$ and $T4$ and the absence of $T3$, in contrast with the RB model predictions and the results on the CVD-grown samples, which might be characteristic of the technique.

5. PECVD and Ph-CVD SiN films

ERDA measurements estimate that the PECVD1, PECVD2, and Ph-CVD samples have significant hydrogen content (22.6%, 16%, and 26.6%, as listed in Table II), and therefore the consideration of hydrogen-containing tetrahedra for a correct fitting of the dielectric function is necessary. RBS measurements calculate that the corresponding [N]/[Si] ratios for the above samples are 0.95, 1.3, and 1.25, respectively.

From the above data, samples PECVD1 is supposed to be silicon and hydrogen rich, which indicates the existence of a considerable number of Si-Si as well as Si-H bonds, and therefore the $\text{Si-Si}_{4-v}\text{N}_v$ and $\text{Si-N}_{4-v}(\text{NH})_v$ tetrahedra are inadequate for a precise description of the material. Moreover, the significant amount of hydrogen (26.6%) in the Ph-CVD sample cannot exclude the presence of some Si-H bonds, and therefore our description, which does not involve the above bonds, cannot be very accurate in this case. On the other hand, sample PECVD2 is reported to be near to stoichiometric ([N]/[Si]=1.3) with a relatively low hydrogen content, which can denote that Si-H bonds may be absent, and thus our description involving $\text{Si-Si}_{4-v}\text{N}_v$ and $\text{Si-N}_{4-v}(\text{NH})_v$ tetrahedra must be suitable in this case. From all the above it is evident that the fitting results for the PECVD1 and Ph-CVD samples are not expected to be reliable.

The best-fit results for these three samples are listed explicitly in Table IV. Common features are the absence of tetrahedron $T3$, and the presence of tetrahedra $T2$ and $T1H$ in all cases. The dielectric responses of tetrahedra $T4$ and $T1H$ are similar and have broad structure, and therefore the fitting program cannot easily distinguish between these two contributions. The estimated void fractions are rather high (25–32 %), which may be indicative of inferior film quality. The estimated [N]/[Si] ratio for the case of sample PECVD1 is quite surprisingly very near the RBS/NRA result, although the hydrogen content is calculated to be very low (10.9%), as expected. The [N]/[Si] ratio for samples PECVD2 and Ph-CVD is estimated to be systematically lower than the corresponding RBS/NRA results. Yet the hydrogen content of sample PECVD2, which as explained above is the most suitable for a tetrahedron analysis, is estimated to be 13.1%, very near the ERDA result and within the error limits of the techniques (±10%).

C. Discussion: stoichiometry and quality of SiN thin films

The $T3$ tetrahedron is found to be present in all films prepared by the CVD technique, and absent in all other films. The existence of tetrahedra $T2$, $T3$, and $T4$ in the CVD films and the ratios between the corresponding tetrahedron volume fractions are indicative of random bonding and hence superior material quality. On the other hand, the absence of $T3$ in the case of all other types of SiN films (PVD, SP, etc.) suggests the existence of nonhomogeneity, i.e., nonrandom distribution of the Si-Si and Si-N bonds, within the material. This superiority of the

TABLE IV. Composition and stoichiometry of the PECVD and Ph-CVD SiN films, as determined from the tetrahedron-model analysis of the dielectric function by considering $\text{Si-Si}_{4-v}\text{N}_v$ and $\text{Si-N}_{4-v}(\text{NH})_v$ tetrahedra.

	Tetrahedron volume fractions (%)						Void fraction	Atom fractions (%)			
	$T1$	$T2$	$T3$	$T4$	$T1H$	$T2H$	(%)	Si	N	H	[N]/[Si]
PECVD1	7.5	33.5		1.4	57.6		31.7	49.9	40.8	9.3	0.82
PECVD2		26.9			73.1		25.4	43.4	44.6	12.0	1.03
Ph-CVD		29.6		6.5	39.2	24.7	30.7	43.4	43.5	13.1	1.00

CVD technique is probably due to the nature of the technique itself, nevertheless, a detailed study of the above is beyond the scope of this work.

From the dielectric-function curves of Figs. 3 and 4 a relationship can be established between the [N]/[Si] ratio $(1-x)/x$ and the energy position of the maximum $\varepsilon_{2\max}$ of the dielectric function $\varepsilon_2(\omega)$. In Fig. 6 we present this relation for randomly bonded (solid line) and phase-separated materials, which consist of Si and Si_3N_4 distinct phases (dashed lines). As already noted in Sec. III B, for the PS case two peaks are observed for intermediate nitrogen concentrations, hence two dashed lines appear in Fig. 6. The existence of a PS volume fraction in a RB material causes a broadening of the ε_2 main peak and a shift of the $\varepsilon_{2\max}$ location toward high (low) energies for high (low) nitrogen concentration.

The tetrahedron model analysis of the dielectric function enables the determination of the [N]/[Si] ratio in SiN materials. In Fig. 6 is shown the energy location of $\varepsilon_{2\max}$ for all films studied versus the [N]/[Si] ratio, as predicted by the RBS/NRA techniques (solid circles) and the tetrahedron model (open circles). It is noticeable that for a variety of SiN films which exhibit $\varepsilon_{2\max}$ ranging between 8.0 and 8.6 eV, RBS/NRA proposes that [N]/[Si]=1.3, identical for all samples, whereas ERDA measurements estimate low hydrogen concentration (below 7%). The same is evident in the case of PVD films, which are reported by RBS/NRA to have [N]/[Si]=1.0, although their $\varepsilon_{2\max}$ differs greatly. The existence of hydrogen up to 15% in these films cannot explain this discrepancy. The Si-H and N-H bonds which must be formed in this case absorb at higher energies than the Si-Si and Si-N bonds, respectively, and therefore cause a shift of the $\varepsilon_{2\max}$ toward higher energies. The tetrahedron-model predictions lie closer to the theoretical curve (solid line) than the RBS/NRA predictions at the region [N]/[Si]>1.10. The deviation between the two predictions is below 15%, which is acceptable, since the error limit of the RBS/NRA technique is around 5–10%. Moreover, ASP estimations of the [N]/[Si] ratio of the DN1 and DN3 samples propose that [N]/[Si] equals 1.66 and 1.9, respectively,[32] which is in big discrepancy with the RBS/NRA and tetrahedron-model values (see Table II), and which has been attributed to possible preferential sputtering.[33,34]

The broadening of the main peak of the dielectric function ε_2 is supposed to consist of the case of a-Si_3N_4 (Ref. 17) entirely of the $T4$ tetrahedron. The application of the dispersion relations proposed by Forouhi and Bloomer[35] (see the Appendix, Sec. 1) estimates it at around 2.8 eV. All other tetrahedra exhibit maximum dielectric response (i.e., $\varepsilon_{2\max}$) at lower energies. Therefore, the existence in a SiN film of other tetrahedra except $T4$, such as $T3$ and $T2$, at non-negligible amounts, is expected to increase the broadening Γ_0 of the main absorption peak, as well as to lower its energy location ω_0, which is directly associated with $\varepsilon_{2\max}$. The ratio of the sum of all other volume fractions over the volume fraction of tetrahedron $T4$, i.e., the quantity $(u_0+u_1+u_2+u_3)/u_4$ which equals $(1-u_4)/u_4$, seems to be appropriate for such a description. In Fig. 7 we present the dependence of this parameter, as estimated from the tetrahedron-model analysis (see Tables III and IV), versus the broadening Γ_0, as determined from the analysis with the macroscopic model of Eqs. (A1a) and (A1b) (Appendix, Sec. 1). For the case of PECVD and Ph-CVD films we apply the ratio $(1-u_4-u_{1H})/(u_4+u_{1H})$ for a consistent description. Each solid circle in Fig. 7 represents one SiN film, and the dashed line acts as a guide to the eye by showing the general trend. The open triangle designates the corresponding point for the $T4$ tetrahedron ($u_4=1, \Gamma_0=2.28$ eV).

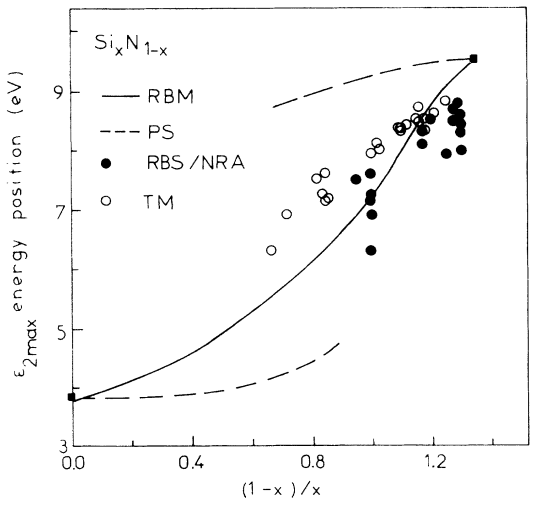

FIG. 6. Energy position of the ε_2 maximum, as determined by SR ellipsometry, vs the [N]/[Si] ratio, as estimated by RBS/NRA (solid circles) and the tetrahedron model (open circles) for various SiN films. The solid and dashed lines show the calculated values, according to the RB and PS models, respectively.

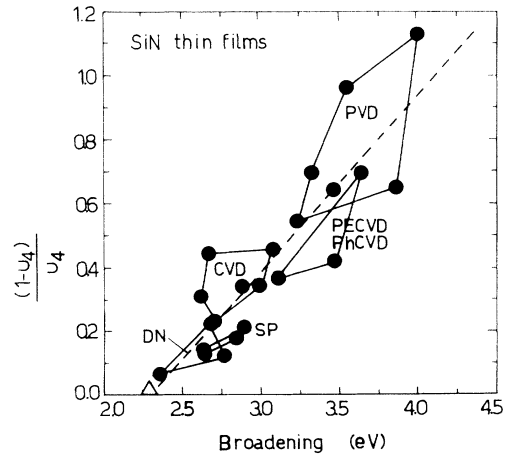

FIG. 7. The $(1-u_4)/u_4$ ratio, as determined by the tetrahedron model, vs the broadening Γ_0, as estimated from Eqs. (A1a) and (A1b), for various SiN films (solid circles). The polygons connect samples prepared by the same growth technique, and the dashed line acts as a guide to the eye. The open triangle designates the corresponding point for the $T4$ tetrahedron.

From Fig. 7 there seems to exist an almost linear relationship between the quantities $(1-u_4)/u_4$ and Γ_0, which implies that they are both indicative of the energy range at which the oscillator strength for the interband electronic transitions is concentrated and can be characteristic of the material quality. The polygons in the same figure include the samples prepared by the same growth technique. It is noticeable that the various techniques yield samples which occupy different regions in this diagram. At first sight this must be associated with the overall [N]/[Si] ratio, since the nitrogen-deficient PVD samples are located together at the upper part of Fig. 7. However, the actual values of Γ_0 and $(1-u_4)/u_4$ depend not only on the stoichiometry, but also on the number of existing tetrahedron types, as well as on their respective volume fraction ratios. For instance, the SP and DN films, which are practically comprised of two tetrahedra ($T2$ and $T4$), exhibit small broadenings, whose differences depend on the respective u_2/u_4 ratios. Moreover, materials that exhibit homogeneous distribution of Si-Si and Si-N bonds, such as the CVD0-4 films, are located at the left-hand side of the dashed line and hence show smaller broadenings than expected, because the $\varepsilon_{2\max}$ locations of their predominant tetrahedra ($T3$ and $T4$) are very close in energy.

The hydrogen-rich PECVD and Ph-CVD films follow the general trend and are located at the right-hand side of the dashed line, because they exhibit higher broadening values than expected. The latter is easily explainable, since in these films the existence of tetrahedron $T1H$ has been established, whose dielectric response is dominant higher in energy than $T4$, and therefore the inclusion of a significant u_{1H} volume fraction instead of a u_4 fraction in EMT calculations that involve tetrahedron $T2$ (see Table IV) yields broader structures. From the above analysis the quantities $(1-u_4)/u_4$ and Γ_0 seem to be characteristic of the technique applied and complementary to each other, and provide an estimation of the stoichiometry and a picture of the dispersion of the tetrahedra that constitute the material.

The goal of SiN growth techniques is to produce dense and stoichiometric material. A criterion of the material density is the void fraction, i.e., as estimated by an EMT analysis, whereas a criterion of the composition may be the energy location of the Penn gap. In Fig. 8 we present the void fraction, which is deduced by the tetrahedron-model analysis, versus the Penn gap energy ω_0, which is determined by fitting of the experimental spectra with Eqs. (A1a) and (A1b) (Appendix). Each circle in Fig. 8 represents one SiN film, and the dashed line acts as a guide to the eye by showing the general trend. One can observe an almost linear relationship between these two quantities, with an upper limit indicated by the open triangle, which corresponds to tetrahedron $T4$ ($\omega_0=8.66$ eV, void fraction $=0$), in good agreement with the general trend. The polygons and lines in Fig. 8 connect samples grown under similar deposition conditions, whereas the labels designate their corresponding origin. Moreover, the CVD sample CVD5, which was obtained from a different source compared to the rest, is located at a different region. This film (indicated by the open circle) is isolated from the rest of the CVD films (designated in Fig. 8 as CVD). The above suggest that the quality and stoichiometry of the resulting CVD films are interrelated, and depend on the preparation technique and possibly the growth conditions implemented.

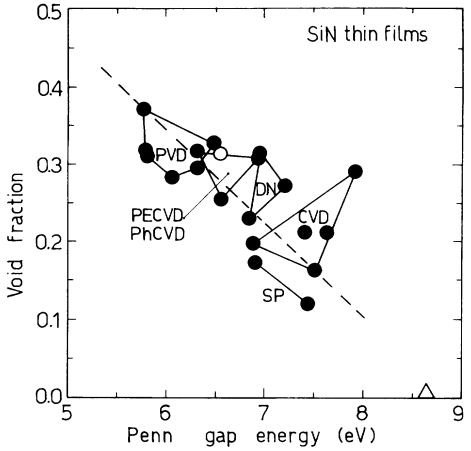

FIG. 8. The void fraction, as determined by the tetrahedron model, vs the Penn gap energy, as estimated from Eqs. (A1a) and (A1b), for various SiN films (solid circles). The open circle designates the CVD5 SiN film, which is located apart from the rest of the CVD SiN films. The polygons and lines connect samples prepared under similar growth conditions, and the dashed line acts as a guide to the eye. The open triangle designates the corresponding point for the $T4$ tetrahedron.

V. THE EFFECT OF HYDROGEN ON THE OPTICAL GAPS OF SiN

The role of hydrogen in a-Si:H is becoming understood, since it is thought to passivate dangling bonds and reduce the density of states in the gap. Moreover, the Si-H states which are estimated to lies 4.0 eV lower than the Si-Si ones[36] cause a recession of the VB top[37] and thus increase the fundamental gap of a-Si:H.[38] On the other hand, the situation in SiN is more complicated, since many types of bonds are involved, and depends on the way H is bonded in the material. The effect of hydrogen is often examined through annealing studies, which are thought to cause hydrogen effusion, bond rearrangement, and densification of the material.[39] For PVD SiN films ([N]/[Si]=1.0), which contained 15% hydrogen and thus a significant number of Si-H bonds, it has been found[40] that annealing causes a shift of the fundamental gap toward higher energies, which implies that the existent Si-H bonds were substituted with Si-N bonds that absorb at higher energies. The opposite behavior has been observed in a-Si:H,[38] which suggests the substitution of Si-H bonds with Si-Si ones that absorb at lower energy.

In order to investigate the effect of hydrogen on the fundamental gap of SiN, we estimated the so-called Tauc gap E_T through the relation[41]

$$\omega.\varepsilon_2^{1/2}=B.(\omega-E_T) \tag{10}$$

for the SiN films which are close to stoichiometric, as

determined by RBS/NRA measurements. Therefore in Fig. 9 we present the dependence of E_T on the hydrogen concentration H%, as estimated by ERDA, for all samples with [N]/[Si] between 1.25 and 1.3, as estimated by RBS/NRA (see Table II). There seems to exist a linear relationship between E_T and H%, which is denoted by the solid line. The Tauc gap decreases with increasing hydrogen and therefore a subsequent hydrogen effusion, i.e, caused by annealing experiments, is expected to increase the value of E_T, in agreement with Ref. 40.

Photoemission and x-ray photoemission spectroscopy (XPS) studies on hydrogenated SiN suggest that for material close to stoichiometric the formation of N-H instead of Si-H bonds is favored[8,9] whose bonding level is estimated to lie 10 eV lower than the VB maximum. Similarly to *a*-Si:H, the conduction-band (CB) minimum is believed to be insensitive to the presence of hydrogen,[10] since the Si-H antibonding states lie at similar energy to the Si-Si ones, which determine the CB minimum. In the Si-rich region ([N]/[Si] < 1) hydrogen is believed to increase the fundamental gap, whereas in the N-rich region ([N]/[Si] > 1) it is thought to have little effect,[10] since the VB edge is mainly determined by the N $p\pi$ states. On the other hand, the decrease of E_T with increasing hydrogen (Fig. 9) can be attributed to the presence of Si-H bonds in the materials under consideration: Since the [N]/[Si] ratio is estimated to be around 1.3, the presence of Si-Si bonds is negligible. Therefore, the observed dependence of E_T must imply that an important amount of Si-H states which lie near the top of the valence band must still be present, and that they determine the band edges. This is evident in the case of the hydrogen-rich sample PECVD2 (H=22.6%, Table II), which exhibits a very low E_T value, apparently due to the large density of Si-H states. Additional Raman spectroscopy measurements in the regions of silicon-hydrogen and nitrogen-hydrogen stretching vibrational modes on samples having [N]/[Si] $\approx$ 1.3 (such as PECVD2 and Ph-CVD) verified the existence of Si-H bonds in the materials.

The presence of hydrogen also affects the mean optical gap of SiN films. It is established in the literature that the center of gravity of the VB DOS is gradually lowered with increasing nitrogen content, since the N $2p_z$ and N $2p_{xy}$ orbitals lie lower than the Si $3p$ level, which determines the mean optical gap in *a*-Si.[21] Hydrogen may shift the center of gravity of the VB DOS toward higher or lower energies, depending on the way it is bonded in the material. It has been determined[8] that Si-H and N-H bonding states lie at 6.3 and 9.8 eV lower than the VB maximum, whereas the Si-N bond is sited between these values, as seen from the dielectric-function spectra of the $Si\text{-}Si_{4-v}H_v$, $Si\text{-}Si_{4-v}N_v$, and $Si\text{-}N_{4-v}(NH)_v$ tetrahedra.[27,30] Therefore, the incorporation of hydrogen in Si-H bonds is expected to raise the center of gravity of the VB DOS and consequently lower the mean optical gap, whereas the formation of N-H bonds is anticipated to have different effects.

The dependence of the energy position of ε_{2max} on the hydrogen concentration, as determined by ERDA, is presented in Fig. 10. Every point shown in the graph corresponds to one SiN film, and only samples having [N]/[Si] between 1.25 and 1.30, as determined by RBS/NRA, are included. The solid line represents the data fit according to a linear model. From Fig. 10 a gradual decrease of ε_{2max} with hydrogen is observed. Analysis of the dielectric function with the dispersion model of Eqs. (A1a) and (A1b) provides a similar dependence for the Penn gap ω_0 as well. In accordance with the preceding paragraph, this dependence might confirm that Si-H bonds are formed in the materials, and possibly that the concentration of Si-H bonds is greater than that of N-H ones, so that finally the center of gravity of the VB DOS is shifted to higher energies, i.e., nearer to the CB minimum.

Since it is known that at temperatures above 350 °C Si-H bonds are broken, and in an attempt to confirm the above argument, we performed annealing experiments on samples SP1 and DN1. The annealings took place at a temperature of 500 °C for half an hour (our experimental

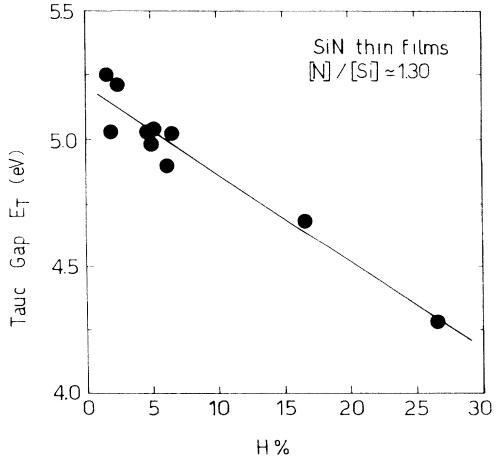

FIG. 9. The Tauc gap, as estimated by Eq. (9), vs the hydrogen concentration, as determined by ERDA, for the SiN films which have [N]/[Si] around 1.3 (as estimated by RBS/NRA).

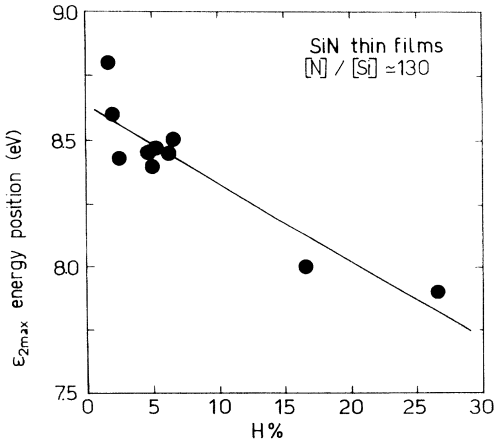

FIG. 10. The ε_{2max} energy position vs the hydrogen concentration, as determined by ERDA, for the SiN films which have [N]/[Si] around 1.3, as estimated by RBS/NRA.

facility did not allow for higher temperatures). Analysis of the dielectric-function spectra showed an increase of ε_{2max} and ω_0 after annealing. This fact suggests that the hydrogen effusion which took place during annealing caused the center of gravity of the VB DOS to shift toward lower energies, and thus that the effused hydrogen formed Si-H bonds in the material. This result is in further agreement with the hydrogen dependence of the ε_{2max} that was described above.

VI. TEMPERATURE DEPENDENCE OF THE OPTICAL GAPS OF SiN

In crystalline materials the temperature-dependent shifts of electronic states are generally the joint effect of two phenomena: the thermal expansion, which induces a small shift to the red, and the electron-phonon coupling, whose influence depends on the material studied. The electron-phonon interaction is calculated from the application of second-order perturbation theory to the electron self-energy, and comprises two contradictory factors: the Debye-Waller and self-energy terms, which cause larger shifts to the red and blue, respectively. On the other hand, in amorphous materials the causes of the observed shifts cannot easily be distinguished due to the absence of translational symmetry. In *a*-Si:H it was found that both fundamental and mean optical gaps are lowered with temperature.[39]

Dielectric-function measurements on SiN bulk materials and thin films were taken in the temperature range 80–700 K. For the determination of the temperature dependence of the mean optical gap three methods have been applied: (i) estimation of the ε_{2max} energy position, directly from the experimental spectra, (ii) fitting of the imaginary part of the dielectric function with the theoretical model proposed by Campi and Coriasso[42] [Eq. (A2)—see the Appendix, Sec. 2] and (iii) fitting of both parts of the dielectric function with the theoretical dispersion relations proposed by Forouhi and Bloomer[29] [Eqs. (A1a) and (A1b)—see the Appendix, Sec. 1].

In Fig. 11 we present the temperature dependence of the mean optical gap of three samples under study, namely PVD4 [Fig. 11(a)], BULK1, and BULK2 [Fig. 11(b)], respectively. Samples BULK1 and BULK2 are in bulk form, hydrogen free, and their stoichiometry ([N]/[Si]) is estimated by RBS/NRA to be 1.0 and 1.3, respectively. The stars, dark circles, and open circles indicate the values of ε_{2max}, ω_{CC} and ω_0 obtained with methods (i), (ii), and (iii), respectively. From these figures a gradual increase of the mean gap with temperature can be verified, which is different to the corresponding shift in *a*-Si. Model (i) seems to provide the most consistent data that have the smallest dispersion. The respective temperature coefficients for samples PVD4, BULK1, and BULK2 are 0.83 (37), 0.76 (17), and 0.15 (13) $\times 10^{-4}$ eV/K, where the number in parentheses designate the 95% confidence limits. From the above it can be seen that these temperatures shifts are small, and become close to zero for the BULK2 SiN sample which is close to stoichiometric ([N]/[Si]=1.3), which indicates that the nitrogen concentration might influence the observed dependence. The results are listed in Table V.

The dependence on temperature of the fundamental absorption of SiN films is studied through the variation of the so-called "E_{03}" gap, which denotes the energy position at which the absorption coefficient rises to around 10^3 cm^{-1}; this position corresponds to the one before the last interference fringe maximum in the dielectric function spectra, and therefore its location is easy to determine. The energy shift of E_{03} with temperature is presented in Fig. 12 for the PVD5 ([N]/[Si]=1.0, H=7%) and CVD 1 ([N]/[Si]=1.3, H=2%) SiN films, respectively. A decrease of the E_{03} gap with temperature is observed for both SiN films. In the case of *a*-Si:H (Ref. 36) a similar trend was found, and was attributed to the presence of hydrogen, which determines the VB edge location.

The temperature coefficients for the SiN PVD5 and CVD1 samples are estimated at 1.75 (22) and 1.55 (39) $\times 10^{-4}$ eV/K, respectively, where the numbers in parentheses indicate the 95% confidence limits (see also Table V). This may be associated mainly with the nitro-

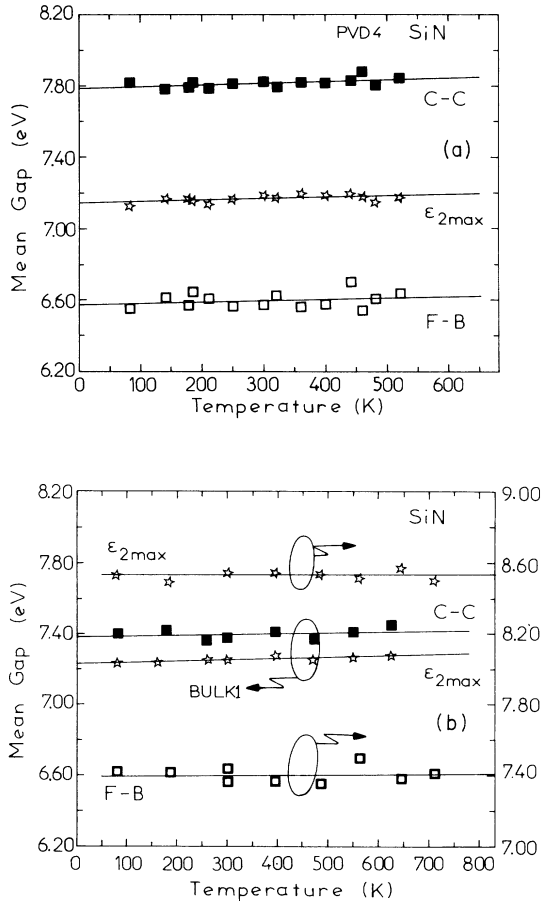

FIG. 11. (a) Temperature dependence of the mean optical gap of the PVD4 SiN thin film, as determined by (i) the ε_{2max} energy position (stars), (ii) analysis of $\varepsilon_2(\omega)$ with Eq. (A2) (dark circles), and (iii) analysis of $\varepsilon(\omega)$ with Eqs. (A1a) and (A1b) (open circles). (b) As in (a), for the BULK1 and BULK2 SiN bulk samples.

TABLE V. Temperature coefficients of the mean optical (here denoted as ω_M) and fundamental (E_{03}) energy gaps of several SiN samples. The numbers in parentheses indicate the 95% confidence limits and stoichiometry data, as determined by RBS/NRA and ERDA, are also presented.

Sample	Deposition technique	[N]/[Si] (RBS/NRA)	H% (ERDA)	$d\omega_M/dT$ (10^{-4} eV/K)	dE_{03}/dT (10^{-4} eV/K)
BULK1	sintering	1.0	0	0.76 (17)	
BULK2	sintering	1.3	0	0.15 (13)	
PVD4	PVD	1.0	8	0.83 (37)	
PVD5	PVD	1.0	5		1.75 (22)
CVD-1	CVD	1.3	2		1.55 (39)

gen content in the films, since *a*-Si and *a*-Si:H were found to exhibit generally higher-temperature coefficients (about 2×10^{-4} eV/K).[39] Although the highest heating temperature was 350 °C, which is the onset of hydrogen effusion, in the case of the PVD5 sample the observed dependence is reversible with respect to increasing or decreasing temperature, which implies that no changes of the hydrogen content took place during the experiments. On the other hand, the CVD1 film was grown at 900 °C, and therefore no hydrogen effusion from Si-H bonds took place during our temperature measurements.

It is generally established for crystalline materials that the more insulating a material, the lower the temperature dependence of its optical gaps, since a higher fundamental gap is known to be accompanied by smaller temperature shifts. This might also happen in the case of the SiN films under study. A possible additional influence of hydrogen on the observed shifts is difficult to distinguish and needs a more systematic investigation.

VII. CONCLUSIONS

In this work we analyze the optical properties of SiN thin films with the tetrahedron model, and thus fit the experimental dielectric-function spectra with respect to Si-centered tetrahedra. By estimating the type and volume fractions of the existing tetrahedra one can deduce, first of all, qualitative results for the efficiency of the applied preparation techniques to produce good-quality films. By analyzing samples prepared by various techniques, it is confirmed that the CVD technique yields films of superior quality and homogeneity. Moreover, a microscopic model is proposed for the determination of the SiN films stoichiometry from the tetrahedron-model data. The results concerning the [N]/[Si] ratio are compared to corresponding ones from RBS/NRA and are found to be in very good agreement. In addition, the optical parameters of the SiN films which are deduced from analysis of the dielectric-function spectra with appropriate models are found to be associated with tetrahedron-model parameters: the mean optical gap energy and broadening are distinctly related to the void and $T4$ tetrahedron volume fractions, respectively, a fact indicating that the two descriptions, with the Forouhi-Bloomer dispersion relations and via the tetrahedron model, are complementary to each other. The exact values of the optical and tetrahedron-model parameters depend on the growth technique implemented and not solely on the nitrogen content in the film, as would be expected.

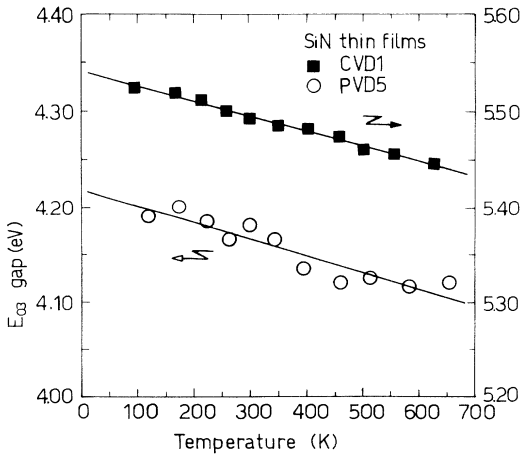

FIG. 12. Temperature dependence of the E_{03} energy gap of PVD5 (open circles) and CVD1 (solid squares) SiN thin films.

Moreover, the fundamental and mean optical gaps of SiN_x:H are found to decrease with increasing hydrogen content for materials close to Si_3N_4, which indicates a shift of the VB to and the VB center of gravity, respectively, toward higher energies. These shifts are in agreement with annealing results reported elsewhere, and can be interpreted by the existence of a significant number of Si-H bonds in the films.

Finally, results are presented for the temperature dependence of the fundamental and mean optical gaps of bulk and thin-film SiN. The former gap is found to be redshifted with temperature and to exhibit temperature coefficients lower than *a*-Si, which decrease with increasing nitrogen in the materials. The latter was modeled in three ways, and an increase with temperature was thus established for all samples studied, in contrast to what is observed in *a*-Si.

ACKNOWLEDGMENTS

This work was partially supported by the EC/LSI [contract No. GE 1-0018-D(B)] and the STRIDE HELLAS 348 projects. The authors wish to thank A. Markwitz for providing RBS/NRA and ERDA results and a number of SiN samples, Dr. S. Boultadakis for performing Raman spectroscopy measurements, and Dr. E. C. Paloura and A. Knop for providing SiN samples.

APPENDIX: DIELECTRIC-FUNCTION MODELING WITH ANALYTICAL EXPRESSIONS

1. The Forouhi-Bloomer model

In an aim to relate the tetrahedron-model results to the optical parameters of SiN, we examine SiN films with the well-known theoretical model proposed by Forouhi and Bloomer,[35] and extended for the case of thin-film structures,[40] which approximates the dielectric response of tetrahedral amorphous semiconductors and insulators and is consistent with the Kramers-Kronig transformation. The analytical expressions for the real and imaginary parts of the refractive index $\tilde{n}(=n+i\kappa)$ according to this model are the following:

$$n(\omega)=n_\infty+\frac{B_0\omega+C_0}{(\omega-\omega_0)^2+\Gamma_0^2} \tag{A1a}$$

and

$$\kappa(\omega)=\frac{A(\omega-\omega_g)^2}{(\omega-\omega_0)^2+\Gamma_0^2}\theta(\omega-\omega_g)\ . \tag{A1b}$$

The model includes the energy ω_0, where the absorption coefficient becomes maximum, which is proportional to the mean distance between the valence and conduction bands and is often called the "Penn gap," and the energy ω_g which accounts for the onset of interband transitions and represents the fundamental gap of the material, or better the energy position at which $\kappa(\omega_g)=0$. The parameter Γ_0 stands for the broadening of the main absorption peak, whereas θ is the Heaviside step function.

The above dispersion relations describe bulk materials and can appropriately be modified for the case of a layered structure configuration, in order to describe thin films. Since almost all SiN films studied in this work are grown on c-Si, we developed a three-phase layered configuration (air-film substrate) and fitted the dielectric-function spectra in an aim to extract the optical parameters included in Eqs. (A1a) and (A1b) and determine the film thickness d.[32] The fits extended over a wide energy range, from well below the fundamental gap to the upper limit of measurement (9.5 eV), and thus included the main absorption peak as well as several interference fringes. In this manner the optical parameters involved can reliably be estimated. The relation between the fundamental ω_g and Penn gap ω_0 in SiN films has been presented in Ref. 32.

2. The Campi-Coriasso model

The model proposed by Campi and Coriasso[42] provides an analytical expression for the imaginary part $\varepsilon_2(\omega)$ of the dielectric function of tetrahedrally coordinated amorphous compounds, with parameters bearing a physical significance. The model is as follows:

$$\varepsilon_2(\omega)=\frac{\omega_p^2}{\omega}\frac{\Gamma(\omega-\omega_g)^2}{[\omega_{0C}^2-(\omega-\omega_g)^2]^2+\Gamma^2(\omega-\omega_g)^2}\theta(\omega-\omega_g)\ . \tag{A2}$$

The parameters ω_p and ω_g stand for the plasma frequency and the fundamental gap of the material. The other two parameters Γ and ω_{0C} are directly related to the electronic density of states and especially to the energy distance between the bonding and antibonding states and the valence-band width. Moreover, Γ determines the broadening of the $\varepsilon_2(\omega)$ peak, as well as the energy separation between the maximum and minimum of the $\varepsilon_1(\omega)$ spectrum, whereas the maximum of $\varepsilon_2(\omega)$, i.e., the mean optical gap ω_{CC}, is located around the energy $(\omega_g+\omega_{0C})$. From Eq. (A2) the real part $\varepsilon_1(\omega)$ of the dielectric function can be calculated with the Kramers-Kronig transformation. This calculation was performed for the SiN films studied in this work, in order to check the self-consistency of the model.

[1] V. Smid, N. M. Dung, L. Stourac, and K. Jurek, J. Non-Cryst. Solids **70**, 1 (1985).
[2] M. J. Powell, B. C. Easton, and O. F. Hill, Appl. Phys. Lett. **38**, 794 (1981).
[3] K. Hiranaka, T. Yoshimura, and T. Yamaguchi, J. Appl. Phys. **62**, 2129 (1987).
[4] K. Domansky, D. Petelenz, and J. Janata, Appl. Phys. Lett. **60**, 17 (1992).
[5] K. Mui and F. W. Smith, J. Appl. Phys. **63**, 475 (1988).
[6] M. Beaudoin, M. Meunier, and C. J. Arsenault, Phys. Rev. B **47**, 2197 (1993).
[7] R. A. Street and C. C. Tsai, Appl. Phys. Lett. **48**, 1672 (1986).
[8] R. Karcher, L. Ley, and R. L. Johnson, Phys. Rev. B **30**, 1896 (1984).
[9] E. Bustarret, M. Bensouda, M. C. Habrard, J. C. Bruyere, S. Poulin, and S. C. Gujrathi, Phys. Rev. B **38**, 8171 (1988).
[10] J. Robertson, Philos. Mag. B **63**, 47 (1991).
[11] A. Knop and U. Doebler (unpublished).
[12] A. Markwitz, H. Baumann, E. F. Krimmel, M. Rose, K. Bethge, P. Misaelides, and S. Logothetidis, Vacuum **44**, 397 (1992).
[13] A. Markwitz, M. Bachmann, H. Baumann, K. Bethge, E. F. Krimmel, and P. Misaelides, Nucl. Instrum. Methods Phys. Res. B **68**, 218 (1992).
[14] E. C. Paloura, J. Lagowski, and H. C. Gatos, J. Appl. Phys. **69**, 3995 (1991).
[15] E. C. Paloura, A. Knop, K. Holldack, U. Doebler, and S. Logothetidis, J. Appl. Phys. **73**, 2995 (1993).
[16] D. E. Aspnes, S. M. Kelso, R. A. Logan, and R. Bhatt, J. Appl. Phys. **60**, 754 (1986).
[17] See, e.g., R. M. A. Azzam and H. M. Bashara, *Ellipsometry and Polarized Light* (North-Holland, Amsterdam, 1977).
[18] S. Logothetidis, J. Petalas, H. M. Polatoglou, and D. Fuchs, Phys. Rev. B **46**, 4483 (1992).
[19] R. L. Johnson, J. Barth, M. Cardona, D. Fuchs, and A. M. Bradshaw, Rev. Sci. Instrum. **60**, 2209 (1989).
[20] J. Barth, R. L. Johnson, and M. Cardona, in *Handbook of Optical Constants of Solids II*, edited by E. D. Palik (Academic, Orlando, FL, 1991), p. 2193.
[21] E. A. Davis, N. Piggins, and S. C. Bayliss, J. Phys. C **20**, 4415

(1987).
[22]D. E. Aspnes, A. A. Studna, and E. Kinsbrom, Phys. Rev. B **29**, 768 (1984).
[23]H. R. Phillip, in *Handbook of Optical Constants of Solids,* edited by E. D. Palik (Academic, Orlando, FL, 1985), p. 771.
[24]S. Logothetidis, J. Appl. Phys. **65**, 2416 (1986).
[25]H. R. Phillips, J. Non-Cryst. Solids **8-10**, 627 (1972).
[26]D. E. Aspnes and J. B. Theeten, J. Appl. Phys. **50**, 4928 (1979).
[27]Z. Yin and F. W. Smith, Phys. Rev. B **42**, 3658 (1990).
[28]D. A. G. Bruggemann, Ann. Phys. (Leipzig) **24**, 636 (1935); D. E. Aspnes, Thin Solid Films **89**, 249 (1982).
[29]S. Boultadakis, S. Logothetidis, S. Ves, and J. Kircher, J. Appl. Phys. **73**, 914 (1993).
[30]K. Mui and F. W. Smith, Phys. Rev. B **38**, 10 623 (1988).
[31]S. Hasegawa, J. He, T. Inokuma, and Y. Kurata, Phys. Rev. B **46**, 12 478 (1992).
[32]S. Logothetidis, J. Petalas, A. Markwitz, and R. L. Johnson, J. Appl. Phys. **73**, 8514 (1993).
[33]E. C. Paloura, S. Logothetidis, S. Boultadakis, and S. Ves, Appl. Phys. Lett. **59**, 280 (1991).
[34]S. S. Chao, J. E. Tyler, D. V. Tsu, G. Lucovsky, and M. J. Mantini, J. Vac. Sci. Technol. A **5**, 1283 (1987).
[35]A. R. Forouhi and J. Bloomer, Phys. Rev. B **34**, 7018 (1986).
[36]L. Ley, in *Physics of Hydrohenated Amorphous Silicon II,* edited by J. D. Joannopoulos and G. Lucovsky (Springer, Berlin, 1984), p. 61.
[37]D. C. Allan and J. D. Joannopoulos, Phys. Rev. Lett. **44**, 43 (1980).
[38]G. F. Feng, M. Katiyar, J. R. Abelson, and N. Maley, Phys. Rev. B **45**, 9103 (1992).
[39]S. Logothetidis, G. Kiriakidis, and E. C. Paloura, J. Appl. Phys. **70**, 2791 (1991).
[40]J. Petalas, S. Logothetidis, A. Markwitz, E. C. Paloura, R. L. Johnson, and D. Fuchs, Physica B **185**, 342 (1993).
[41]J. Tauc, in *Optical Properties of Solids,* edited by F. Abeles (North-Holland, Amsterdam, 1972), p. 303.
[42]D. Campi and C. Coriasso, J. Appl. Phys. **64**, 4128 (1988).